Journal of Korean Institute of surface Engineering
Vol. 32, No. 3, Jun., 1999

THE SURFACE CHARACTERISTICS OF NITROGEN ION IMPLANTED IRON ALUMINIDES

Han-Cheol Choe

Dept. of Metallurgical Engineering & IAGC Research Institute, Kwang Yang College, Kwang Yang, Chonnam, 545-800, Korea

Abstract

The surface characteristics of nitrogen ion implanted iron aluminides were investigated using various electrochemical methods in H_2SO_4+KSCN and HCl solutions. Nitrogen ion implantation was performed with doses of 3.0×10^{17}ions/cm^2 at an energy of 150keV.

Nitrogen ion implanted iron aluminides increased the corrosion potential and significantly decreased grain boundary activation, the active current density, and passive current density. Nitrogen implanted iron aluminides with Mo increased the corrosion, pitting potential, repassivation potential and $|E_{pit}-E_{corr}|$ value. Whereas, implanted iron aluminides containing boron reduced the pitting and repassivation potential in comparison with nitrogen implanted iron aluminides with Cr and Mo.

Key words : *Nitrogen Ion Implantation, Iron Aluminides, Corrosion Potential, Grain Boundary Activation, Pitting and Repassivation Potential*

1. INTRODUCTION

Iron aluminides are of considerable interest for low to intermediate temperature structural applications in which low cost, low density and good corrosion or oxidation resistance are required. However their application is currently limited by their room temperature brittleness. One of the methods being pursued to improve room temperature ductility is addition of third elements, such as Cr, B, and Mo etc[1]. The ductility of iron aluminides can be substantially improved by increasing the aluminum content from 25 to 28 at % and by adding 2-6 at % chromium. These Cr -modified alloys can be further improved by alloying with Mo[2),3)].

Some investigators[4),5),6)] have sought to improve the wear and corrosion resistance of steel containing Mo and N in acidic solution through the process of nitrogen ion implantation. The mechanism of N and Mo induced passivation involves an anodic dissolution inhibition by NH_4^+ as an acidic pit neutralizer and MoO_4^{2-} as a cation selective layer former. Therefore the steels containing Mo and N in acidic solution have high corrosion resistance due to the synergistic effect

of Mo and N in acidic solution[7].

In this study, the surface characteristics of nitrogen ion implanted iron aluminides were investigated using various electrochemical methods in H_2SO_4+KSCN and HCl solutions.

2. EXPERIMENTAL

Fe-28Al materials containing Mo, Cr and B were prepared under hydrogen and in a vacuum arc furnace, respectively, as shown Table 1. The produced materials were heated at 1000℃ under a high purity dried Ar atmosphere and were held at 500℃ for 2 days to stabilize the DO_3 structure of materials[2),6),8].

Nitrogen ion implantation was carried out at the NRIM in Japan. N_2 gas was used as the ion source of the feed materials. Ions were embedded by an accelerator of 150keV with dose of 3.0×10^{17}ions/㎠ on the iron aluminides at 25℃ in 2×10^{-6} torr vacuum. Nitrogen ion implanted surface was investigated by SEM and XRD.

A saturated calomel electrode as a reference electrode, and high density carbon electrode as a counter electrode, were set according to ASTM G5-87[2]. The potentials were controlled at a scan rate of 100mV/min. by a potentiostat (EG&G Instruments Model 273A) connected to a computer system. The various electrochemical methods included the use of the follow in electrolytes : 0.1M H_2SO_4+0.1M KSCN for grain boundary activation, 0.1M HCl for pitting corrosion, and 0.1M H_2SO_4+0.1M HCl for passive film stability. After each electrochemical measurement, the corrosion surface of each sample was investigated by SEM and EDX.

Table 1. Chemical Composition of N_2^+ unimplanted (N_2^+ implanted) Iron Aluminides.

Materials	Chemical Composition (at%)				
	Al	Cr	Mo	B	Fe
FA (NFA)	28	-	-	-	Bal.
FA2C (NFA2C)	28	2	-	-	Bal.
FA6C (NFA6C)	28	6	-	-	Bal.
FA2CM (NFA2CM)	28	2	1	-	Bal.
FA6CM (NFA6CM)	28	6	1	-	Bal.
FAB (NFAB)	28	-	-	0.02	Bal.
FA2CB (NFA2CB)	28	2	-	0.02	Bal.
FA6CB (NFA6CB)	28	6	-	0.02	Bal.

3. RESULTS AND DISCUSSIONS

3.1 Surface Structure of Nitrogen Ion Implanted Iron Aluminides

Fig. 1 show the SEM photography and an XRD pattern of N_2^+ implanted iron aluminides surface (NFA6C) which appears a little roughness and damage resulting from the high dose implantation[6]. The high dose implantation involves the bombardment of ions into the target substrate and certain damage of the surface layer occurs. The damage layer is a few tens or hundreds of nanometers[9] and the damage is in the form of dislocation loop and dislocation arrays. Metastable or stable phases, such as γ'-Fe_4N, α''-$Fe_{16}N$, and metastable Al_6Fe etc[9], are formed during ion implantation by radiation enhanced diffusion. These metastable phase transform to Fe_4N and Al_3Fe on annealing at higher temperatures for sufficient times, for example, α''-$Fe_{16}N$ transforms to γ'-Fe_4N during annealing treatment at 200℃ for 6hr. The analysis of XRD confirms that implanted N combines with Cr, Fe and Al, followed by the formation of metastable nitride [AlN, $Fe_{16}N_2$][10], CrN, Cr_2N, and Fe_4N on the surface[6].

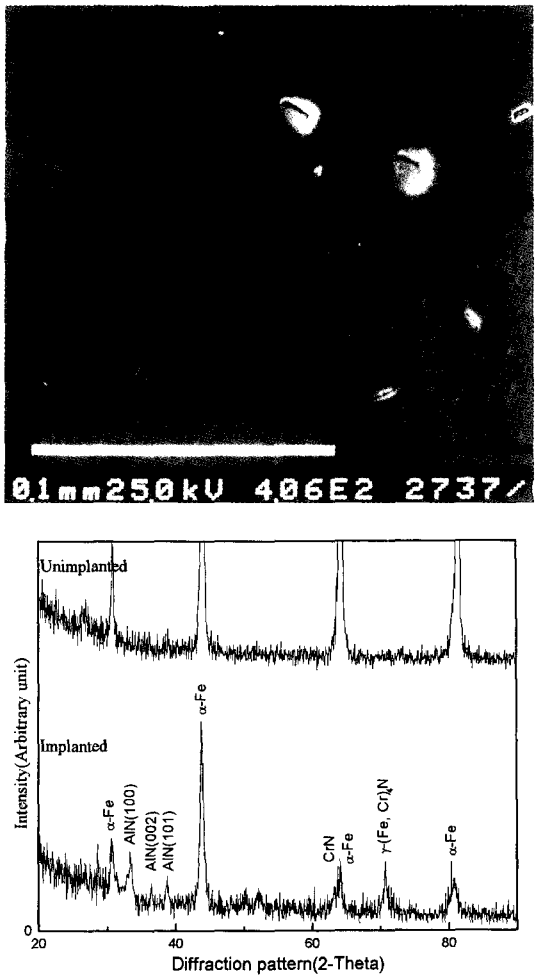

Fig. 1 SEM micrographs and XRD pattern showing N_2^+ implanted surface of iron aluminides (NFA6C).

3. 2 Grain Boundary Activation of Nitrogen Ion Implanted Iron Aluminides

EPR curves were obtained with the aim of evaluating the influence of grain boundary activating agents on IG corrosion[6]. Fig. 2 shows EPR curves obtained in 0.1M H_2SO_4+ 0.1M KSCN solution for N_2^+ implanted and unimplanted iron aluminides. The reactivation and activation current density of N_2^+ implanted iron aluminides were consistently lower than those of N_2^+ unimplanted iron aluminides. The activation and reactivation current density of N_2^+ implanted NFA2CM are 7.0×10^{-3}A/cm^2 and 2.0×10^{-4}A/cm^2, respectively, whereas those of the unimplanted FA2CM are 6.0×10^{-2}A/cm^2 and 5.0×10^{-2} A/cm^2 as shown in Table 2. This decrease in activation current density is caused by the effects of N and Mo, that is, the probable interpretation of this was the presence of Mo in the form of MoO_4^{2-} over the specimen surface in the electrolyte solution to suppress corrosion with SCN^- and to promote passivation[6]. The corrosion potential of the N_2^+ implanted specimen is comparatively high, especially, corrosion potential of N_2^+ implanted iron aluminides containing Mo shows -

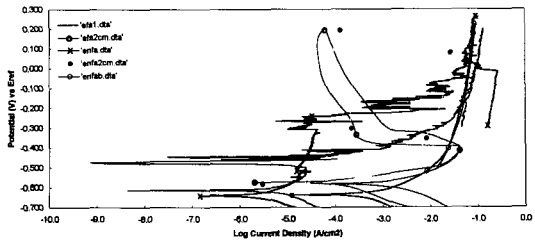

Fig. 2 EPR curves for N_2^+ implanted and N_2^+ unimplanted iron aluminides in 0.1M H_2SO_4+ 0.01M KSCN solution at 25℃.

Table 2 Grain boundary activation data for N_2^+ implanted and unimplanted iron aluminides from EPR curves.

	E_{corr} (mVvs SCE)	I_a (A/cm^2)	I_r (A/cm^2)
FA	-650	N·D	N·D
FA6C	-630	N·D	N·D
FA2CM	-570	6.0×10^{-2}	5.0×10^{-2}
FA6CB	-620	N·D	N·D
NFA	-650	2.0×10^{-5}	2.0×10^{-1}
NFA6C	-630	1.5×10^{-2}	4.0×10^{-2}
NFA2CM	-580	7.0×10^{-3}	2.0×10^{-4}
NFA6CB	-610	3.5×10^{-2}	9.0×10^{-2}

580mV. Unlike the case for Mo addition, the corrosion potential shifted toward the less noble side and both the activation current density and reactivation current density increased significantly in the case of N_2^+ implanted iron aluminides containing boron. The probable explanation for this phenomena is the boride formation at the grain boundary or in the grain[2].

Fig. 3 presents SEM photos of N_2^+ implanted iron aluminides after the intergranular corrosion test. Fig. 3(a) NFA2C and Fig. 3(c) NFA6CB show that the specimen is corroded in the area

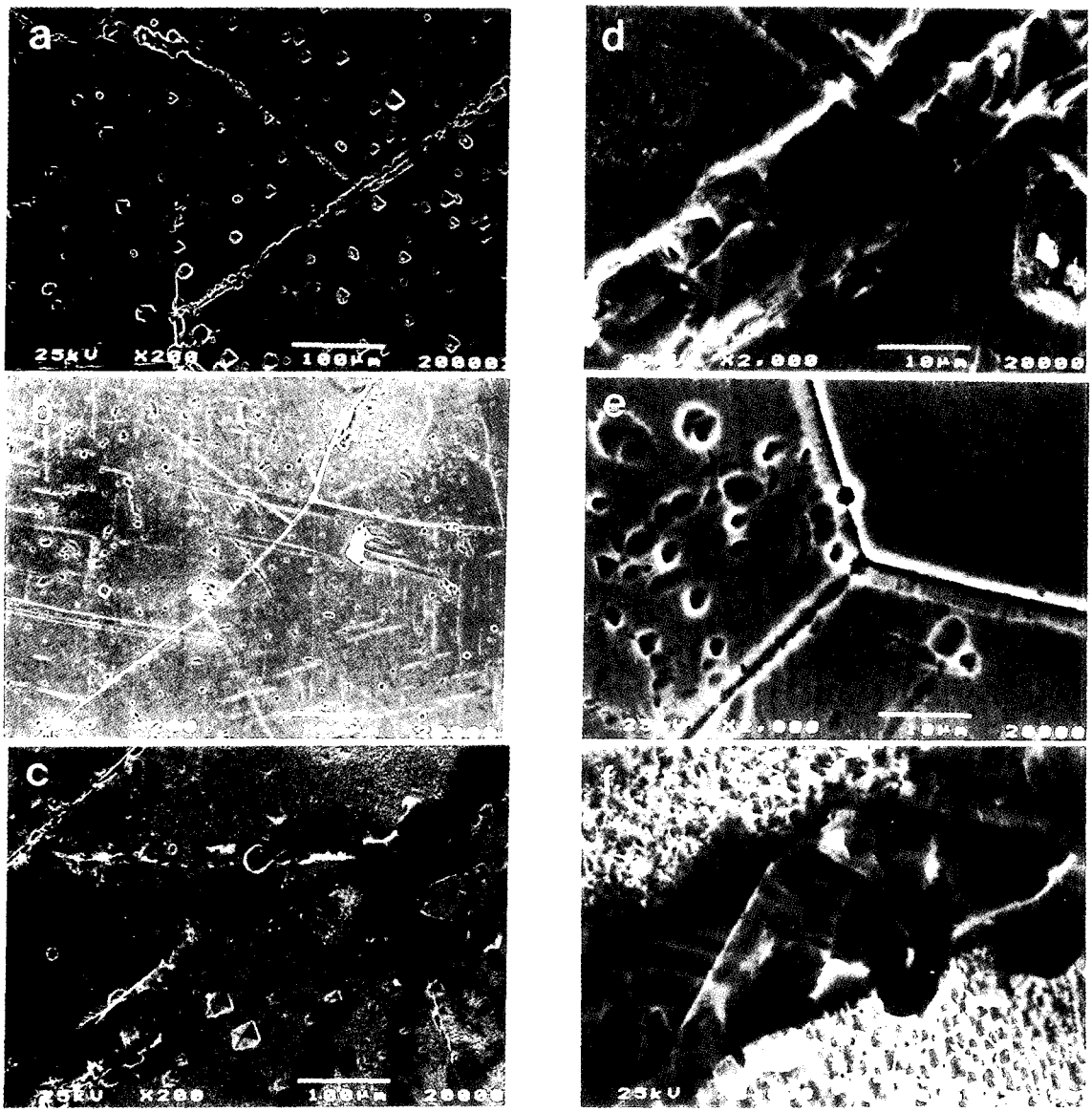

Fig. 3 SEM micrographs showing intergranular corrosion behavior of N_2^+ implanted iron aluminides after EPR testing in 0.1M H_2SO_4+0.01M KSCN solution at 25℃.
(a) NFA2C (b) NFA2CM (c) NFA6CB (d) NFA2C ×2000 (e) NFA2CM ×2000 (f) NFA6CB ×2000

adjacent to the grain boundaries by SCN^-, which complies with EPR curves. The N_2^+ implanted NFA2CM surface (b) is nearly intact, which implies that it is immune to SCN^- which causes pitting corrosion such as halogen ions and this favorable effect of Mo and N was thought to be due to the inhibited penetration of aggressive an ionic species, such as SCN^- and Cl^- by the MoO_4^{2-} and NH_4^+ formed from the dissolved Mo and N[6]. However, In the case of N_2^+ implanted iron aluminides containing B, pitting and intergranular corrosion appeared to be stimulated; this indicated corrosion readiness of the surroundings of the boride precipitate existing along the grain boundary by SCN^-. Fig. (d), (e) and (f) show the magnified photos (×2000) of (a), (b) and (c) surface. We can see the precipitates, such as M_2B, $M_{23}B$, M_2N, $M_{23}N$, AlN etc[6),10)], in the grain and at the grain boundary. And it can be confirmed that the corrosion product is a Al_2O_3 and Cr_2O_3 oxide film[2)] from the results of an EDX analysis of Cr, Al and Fe as shown in Fig. 4.

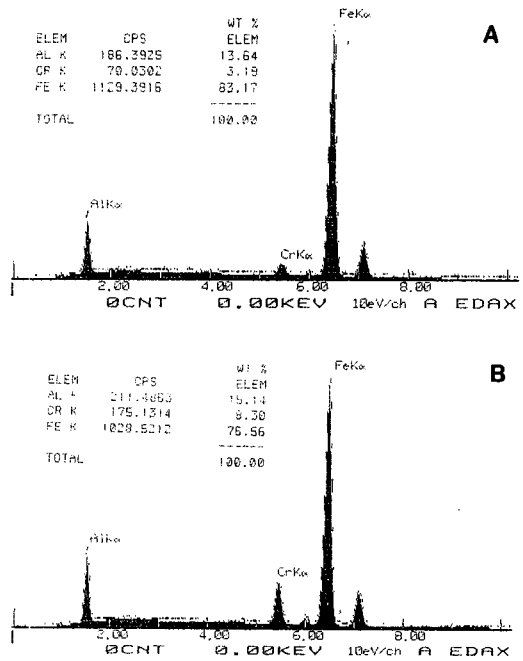

Fig. 4 EDX analysis of corrosion products on NFA2C(a) and NFA6CB(b) iron aluminides surface after EPR testing in 0.1M H_2SO_4+0.01M KSCN solution at 25℃.

3. 3 Pitting Corrosion Behavior of Nitrogen Ion Implanted Iron Aluminides

Fig. 5. summarizes the CPPT curves of N_2^+ implanted and unimplanted iron aluminides obtained in 0.1M HCl solution. The pitting potential of N_2^+ implanted iron aluminides is more drastically increased than that of the unimplanted iron aluminides. In addition, the CPPT curves of N_2^+ implanted samples move to the left and upwards, which causes excellent pitting resistance. The reasons why N_2^+ implanted NFA2CM sample has better corrosion resistance than unimplanted FA2CM sample like Fig. 5 are as follows. There is a synergistic effect between Mo and the implanted N, and secondly, it is thought that MoO_4^{2-} and NH_4^+ ions generated as corrosion products on the surface play an important role in preventing the ingress of Cl^- and act as a pitting inhibitor against the aggressiveness of Cl^- as shown bipolar model[12)] of Fig. 6, that is, dissolved Mo existed in the solution as MoO_4^{2-} and this in turn formed an anion selective layer at the outmost surface of the surface layer. As a consequence, penetration of the Cl^- ion was suppressed and thus the corrosion inhibition effect was raised[6)]. The $|E_{pit}-E_{corr}|$ values of the N_2^+ implanted NFA2CM and NFA6CM samples are higher than that of the implanted iron aluminides without Mo due to the synergistic effect of Mo and N. We see

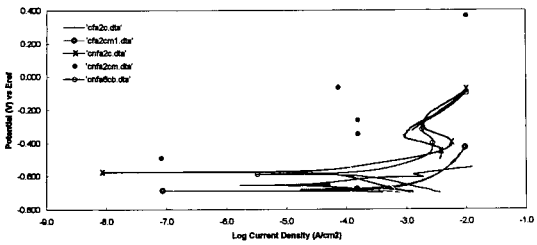

Fig. 5 CPPT curves for N_2^+ implanted and N_2^+ unimplanted iron aluminides in 0.1M HCl solution at 25℃.

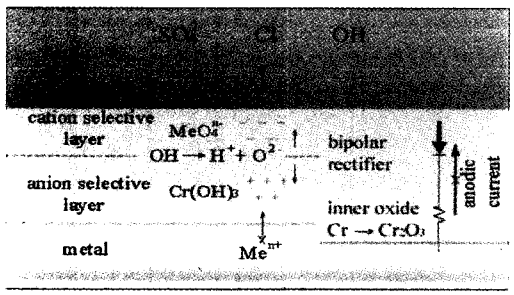

Fig. 6 Schematic representation of the bipolar behavior of the passive film formed on the metal surface(positive charge: +, negative charge: -)

that addition of B causes a shift of the potential towards the less noble side, while the influence of alloying of B was trivial for the pitting potential and repassivation potential. From the observed influence of the B addition, the following mechanism with B estimated: B present in the NFA6CB dissolved into the solution as $B_4O_7^{2-}$ and this ion functions as the pitting inhibitor against $C\ell^{-}$[2]. Table 3 summarizes the results obtained for corrosion potential, pitting potential and repassivation potential of N_2^+ implanted and unimplanted iron aluminides obtained in 0.1M HCl solution.

Fig. 7 shows SEM photos of N_2^+ implanted iron aluminides after CPPT. The pit size of NFA2CM

Table 3 Pitting corrosion data of N_2^+ implanted iron aluminides from CPPT curves.

	Pitting potential E_{pit} (mV vs SCE)	Repassivation potential E_{rep} (mV vs SCE)	Corrosion potential E_{corr} (mV vs SCE)	$\lvert E_{pit}-E_{corr} \rvert$	I_p
NFA	-300		-590	290	7.0×10^{-3}
NFA2C	-240	-265	-575	335	2.0×10^{-3}
NFA6C	-160	-230	-570	410	6.0×10^{-3}
NFA2CM	-25	-260	-480	455	8.0×10^{-3}
NFA6CM	-60	-260	-440	380	3.0×10^{-3}
NFAB	N·D	N·D	-585	-	N·D
NFA2CB	-290	N·D	-600	310	1.5×10^{-3}
NFA6VB	-270	-270	-580	310	1.5×10^{-3}

(b) is small in compared with (a) and (c) of implanted iron aluminides without Mo addition. It can be confirmed that Mo and N act as a pitting inhibitor in chloride solution. In the case of N_2^+ implanted iron aluminides containing B, round pit[13] emerged in compared with irregular pit shape of (a) and (b). It might be interpreted in terms of the $B_4O_7^{2-}$ existed in the pit.

Fig. 8 and 9 shows the potential and current - time curves of N_2^+ implanted and unimplanted iron aluminides in 0.1M H_2SO_4+0.1M HCl solution. The passive film stability of the N_2^+ implanted NFA2CM sample is higher than that of the unimplanted iron aluminides and implanted iron aluminides without Mo addition from the current and potential-time curves.

The current density for N_2^+ implanted and unimplanted iron aluminides containing B increased, as time increased, due to pit nucleation and propagation at precipitates. Whereas, the current density for N_2^+ implanted iron aluminides

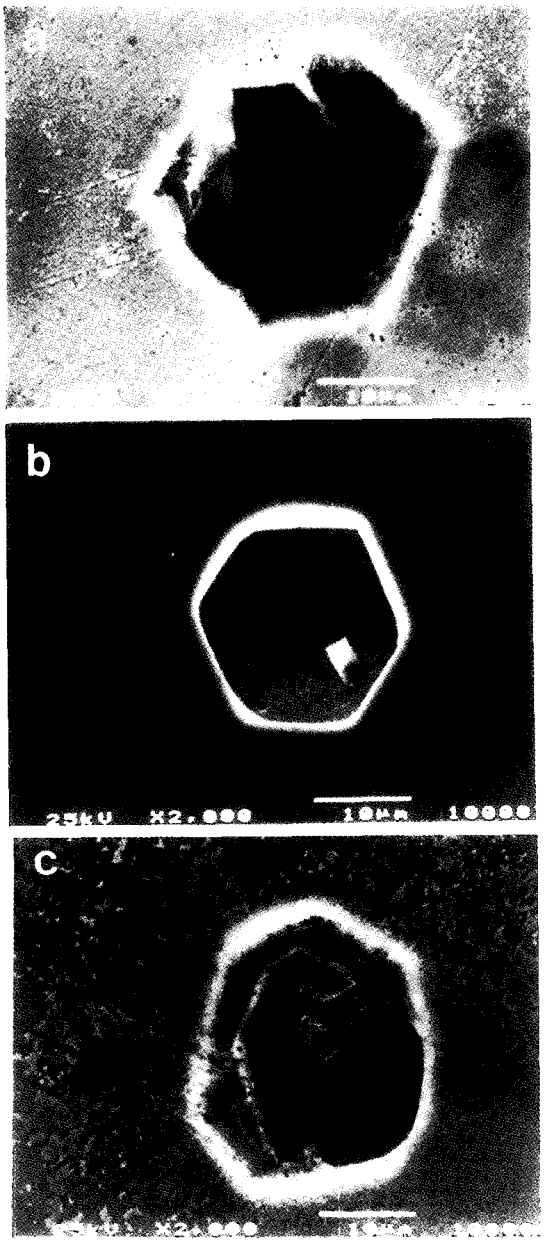

Fig. 7 SEM micrographs showing pitting corrosion behavior of N_2^+ implanted iron aluminides in 0.1M HCl solution at 25℃.
(a) NFA6C (b) NFA2CM (c) NFA6CB

containing Mo drastically decreased, as time increased, due to synergistic effect of Mo and N.

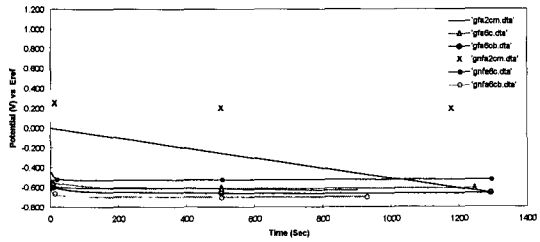

Fig. 8 Potential-time curves for N_2^+ implanted and N_2^+ unimplanted iron aluminides at constant current density(1.0mA/㎠) in 0.1M H_2SO_4+0.1M HCl solution at 25℃.

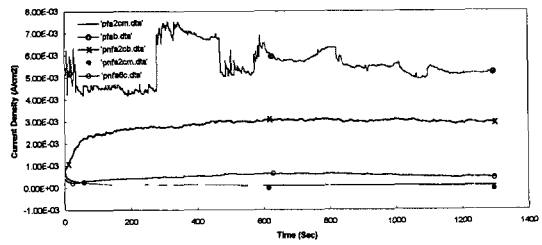

Fig. 9 Current-time curves for N_2^+ implanted iron aluminides at constant potential(100mV) in 0.1M H_2SO_4+0.1M HCl solution at 25℃.

4. CONCLUSIONS

Nitrogen ion implanted iron aluminides increased the corrosion potential and significantly decreased grain boundary activation, the active current density, and passive current density. Nitrogen implanted iron aluminides with Mo increased the corrosion, pitting potential, repassivation potential and $|E_{pit}-E_{corr}|$ value. Whereas, nitrogen ion implanted iron aluminides containing boron reduced the pitting and repassivation potential in comparison with nitrogen implanted iron aluminides with Cr and Mo.

ACKNOWLEDGEMENTS

The author wishes to thank Matsushima of NRIM, Japan, for assistance with the ion implantation.

"This paper was supported by the NON DIRECTED RESEARCH FUND of the Korea Research Foundation, 1997."

REFERENCES

1. B. Schmidt, P. N. Nagpal, and I. Baker, In High Temperature Ordered Intermetallic Aloys III, MRS Symposia Proceedings, MRS, Vol. 133, 755 (1989)
2. H. C. Choe, H. S. Kim, D. C. Choi and K. H. Kim, J. of Materials Science. 32, 1221 (1997)
3. N. S. Stoloff and C. T. Liu, Intermetalllic, 2, 875 (1994)
4. T. Raghu, S. N. Malhotra, and P. Ramakrishnan, Br. Corros. J. 23, 109 (1988)
5. Preston P. Smith and R. A. Buchanan, J. Vac. Sci. Technol., B12 940 (1994)
6. H. C. Choe, Surface and Coatings Technology 112, 299 (1999)
7. R. C. Newman and T. Shahrabi, Corros. Sci., 27, 827 (1987)
8. H. C. Choe, D. C. Choi, K. H. Kim and S. K. Hong, Corrosion Engineering, 45, 137 (1996)
9. Kumar V. Jata and Edgar A. Starke, Jr, J. of Metals, 23 (1983)
10. K. Saito and T. Matsushima, Materials Science and Engineering, A115, 355 (1989)
11. C. K. Lee and H. C. Shih, Corrosion Science, 50, 848 (1994)
12. A. R. Brooks, C. R. Clayton, K. Doss, and Y. C. Lu, 133, 2459 (1986)
13. H. J. Kim, W. B. Carter, R. F. Hochman and E. I. Meletis, Materials Science and Engineering, 69, 297 (1985)